

- vices," in *IEDM Tech. Dig.*, Dec. 1979.
- [3] E. A. Wolsheimer, "Physics, technology and applications of junction charge-coupled devices," Ph.D-thesis, Dep. Elec. Eng., Delft Univ. of Tech., Delft, the Netherlands, 1982.
- [4] —, "Optimization of potential profiles in junction charge-coupled devices," *IEEE Trans. Electron Devices*, vol. ED-28, pp. 811-817, July 1981.
- [5] M. Kleefstra and P. C. Heukemeyer, "Detection of parasitic potential wells or barriers in bulk-transport charge-coupled devices," *Solid-State Electron Devices*, vol. 1, pp. 46-48, Jan. 1977.
- [6] I. Ruge, *Halbleiter-Technology*. Berlin, Germany: Springer, 1975.
- [7] H. F. Wolf, *Silicon Semiconductor Data*. Oxford, England: Pergamon Press, 1969.
- [8] M. J. Howes and D. V. Morgan, *Charge-Coupled Devices and Systems*. Chichester: Wiley, 1979.
- [9] E. A. Wolsheimer, "A parallel-in, serial-out programmable JCCD filter," to be published in *IEEE J. Solid-State Circuits*.
- [10] E. P. May, C.L.M. v.d. Klauw, M. Kleefstra, and E. A. Wolsheimer, "Junction charge-coupled logic," to be published in *IEEE J. Solid-State Circuits*.

## Ion-Sensitive Field-Effect Transistors with Inorganic Gate Oxide for pH Sensing

TATSUO AKIYAMA, MEMBER, IEEE, YUSUKE UJIHIRA, YOICHI OKABE, MEMBER, IEEE,  
TAKUO SUGANO, SENIOR MEMBER, IEEE, AND EIJI NIKI

**Abstract**—Ion-sensitive field-effect transistors (ISFET's) have been fabricated by using silicon films on sapphire substrates (SOS). Using this structure  $\text{SiO}_2$ ,  $\text{ZrO}_2$ , and  $\text{Ta}_2\text{O}_5$  films are examined as hydrogen-ion-sensitive materials, and  $\text{Ta}_2\text{O}_5$  film has been found to have the highest pH sensitivity ( $56 \text{ mV/pH}$ ) among them. The measured pH sensitivity of this SOS-ISFET's is compared with the theoretical sensitivity based on the site-binding model of proton dissociation reaction on the metal oxide film and good agreement between them is obtained.

### I. INTRODUCTION

ION-SENSITIVE FIELD-EFFECT TRANSISTORS (ISFET's), [1]-[10] have a capability of MISFET's combined with an ion-selective electrode. The ISFET's do not have metal-gate electrodes, hence, the electrolyte, in which the ISFET's are immersed, and the reference electrode in the electrolyte, work as the gate electrode. The gate insulator plays the essential role on ion sensing.

Here pH sensitivity of  $\text{SiO}_2$ ,  $\text{ZrO}_2$ , and  $\text{Ta}_2\text{O}_5$  are studied as the gate insulator of ISFET's. So far the pH response charac-

teristics of various materials have been investigated, but the physical and chemical mechanisms of the different pH response characteristics among these materials have not been known. In this paper it is reported that the difference of pH response characteristics is due to the difference between the density of hydroxyl sites on the gate insulator surface and of the proton dissociation reaction.

Furthermore, in order to avoid the technological difficulty in isolating the side walls and the back surface of the ISFET, for preventing the leakage current flowing to the substrate, ISFET's were fabricated with silicon films on the sapphire wafers.

Then the pH sensitivity of these silicon films on sapphire substrates (SOS)-ISFET's was compared with the calculated results based on the site-binding model of proton dissociation reaction on the metal oxide film and a good agreement of pH sensitivity was achieved between them.

### II. THEORY OF pH SENSITIVITY OF OXIDE FILMS

Two mechanisms for the operation of ISFET's were proposed previously. One is that a space-charge layer is formed at the electrolyte-oxide interface and the surface potential of the semiconductor is determined by the space charge. The other is that some species diffuse from the electrolyte to the semiconductor-oxide interface and give influences to change the threshold voltage [11]-[13]. Although the diffusion of chemical species must occur to some extent in ISFET's, it is

Manuscript received March 25, 1982; revised July 9, 1982.

T. Akiyama and Y. Ujihira are with the Department of Industrial Chemistry, Faculty of Engineering, University of Tokyo, 7-3-1, Bunkyo-ku, Tokyo, Japan, 113.

Y. Okabe and T. Sugano are with the Department of Electrical and Electronic Engineering, University of Tokyo, 7-3-1, Bunkyo-ku, Tokyo, Japan, 113.

E. Niki is with the Institute of Vocational Training, 1960, Aihara, Sagamihara-shi, Japan.

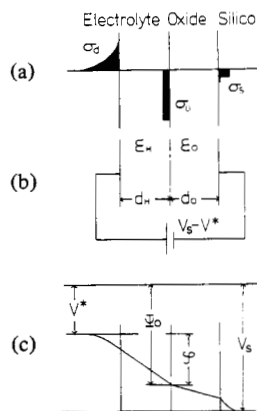


Fig. 1. Charge distribution, capacitance model, and potential profiles of an electrolyte, oxide, and silicon system. (a) Charge distribution. Dipole layer is formed at the interface between the oxide surface and the electrolyte system, where  $\sigma_d$  is the charge per unit area in the Gouy-Chapman space charge region,  $\sigma_0$  is the oxide surface charge per unit area, and  $\sigma_s$  is the semiconductor surface charge per unit area. (b) Capacitance model. The charge distribution can be represented with two capacitors  $C_H$  and  $C_d$  connected in series, where  $C_H = \epsilon_H/d_H$ ,  $C_0 = \epsilon_0/d_0$ ,  $\epsilon_H$  is the dielectric constant of the electric double layer,  $\epsilon_0$  is the dielectric constant of the insulator,  $d_H$  is the thickness of the electric double layer, and  $d_0$  is the thickness of the insulator layer. (c) Potential distribution, resulted from the charge distribution (a).

still questionable whether this process is considered the primary response mechanism or not [14], because rapid response of ISFET's has been observed although the diffusion of chemical species through the oxide must be a slow process. Furthermore, the response of ISFET's should depend on the diffusion constant of chemical species and the oxide thickness, although very small differences in the response time for ISFET's with various oxides have been observed. In fact, Abe *et al.*, have fabricated ISFET's using silicon nitride, silicon dioxide, and silicon oxynitride as the hydrogen-ion-sensitive film [15] and found that silicon nitride ISFET's had the highest pH sensitivity. If the diffusion of protons through the film is the primary mechanism, silicon nitride ISFET's should have a lower sensitivity for pH, because the diffusion constant of proton in silicon nitride is smaller than in silicon dioxide and silicon oxynitride.

Therefore, it is suggested that the response of ISFET's is due to the space-charge formation at the electrolyte-oxide interface rather than due to the diffusion through the film.

At the interface, the interface potential is generated by the process of ion or electron exchange between the electrolyte and the oxide. The charge distribution is illustrated in Fig. 1. Assuming the total charge neutrality, we obtain

$$\sigma_d + \sigma_0 + \sigma_s = 0 \quad (1)$$

where

- $\sigma_d$  charge per unit area in the Gouy-Chapman space-charge region,
- $\sigma_0$  oxide surface charge per unit area, and
- $\sigma_s$  semiconductor surface charge per unit area.

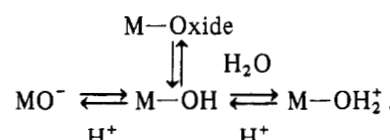
Given the capacitance model, the following equation results:

$$\begin{aligned} \varphi &= \Phi_0 - V^* \\ &= \{\sigma_0 - C_0(V_s - V^*)\}/(C_H + C_0) \end{aligned} \quad (2)$$

where

- $V^* = V_g - V_{ref} + E^0 + (RT/nF) \ln a_i$  [16],
- $V_g$  biased gate potential,
- $\Phi_0$  potential of the oxide surface,
- $V_{ref}$  reference electrode potential,
- $V_s$  potential of the silicon substrate,
- $E^0$  standard electrolyte potential,
- $C_H = \epsilon_H/d_H$ ,  $C_0 = \epsilon_0/d_0$ ,  $\epsilon_H$  dielectric constant of the electronic double layer,
- $F$  Faraday constant,
- $T$  absolute temperature,
- $n$  valency of ions,
- $R$  gas constant,
- $d_H$  thickness of the electronic dipole layer,
- $\epsilon_0$  dielectric constant of the insulator, and
- $d_0$  thickness of the insulator layer.

Now let us consider the oxide surface charge  $\sigma_0$ . When the oxide surface is in contact with an aqueous solution, the surface layer is hydrated to form hydroxyl group [17], [18]. This surface hydroxyl group may be positively charged, negatively charged, or neutral, depending on the pH of the electrolyte. The total charge that can be accommodated on the oxide surface varies by the physico-chemical nature of the surface. Important factors are the surface composition, structure, crystallographic orientation, stoichiometry, and the degree of hydration. Actually, immersing the oxide into the electrolyte, the oxide is often dissolved into the electrolyte. But, neglecting the dissolution of the oxide into the electrolyte, only the surface hydroxyl group is assumed to react with the species of the electrolyte. This Site-Binding Model of the proton dissociation reaction on the metal oxide film can be characterized as follows:



The corresponding electrochemical equations are given by the following equations:

$$\begin{aligned} \mu_{\text{MOH}}^0 + kT \ln v_{\text{MOH}} \\ = \mu_{\text{Mo}^-}^0 + \mu_{\text{H}^+}^0 + kT \ln v_{\text{MO}^-} + kT \ln a_{\text{H}^+} - e\varphi \end{aligned} \quad (3)$$

$$\begin{aligned} \mu_{\text{MOH}_2^+}^0 + kT \ln v_{\text{MOH}_2^+} + e\varphi \\ = \mu_{\text{MOH}}^0 + \mu_{\text{H}^+}^0 + kT \ln v_{\text{MOH}} + kT \ln a_{\text{H}^+} \end{aligned} \quad (4)$$

where

- $\mu_A^0$  standard chemical potential of A's species,
- $v_A$  equilibrium number per unit area of the A's species,
- $a_{\text{H}^+}$  the hydrogen-ion activity,
- $k$  Boltzmann's constant,
- $e$  electronic charge ( $-1.6 \times 10^{-19}$  C), and
- $\varphi$  interface potential between the electrolyte and the oxide.

Then, pH and interface potential are explained as

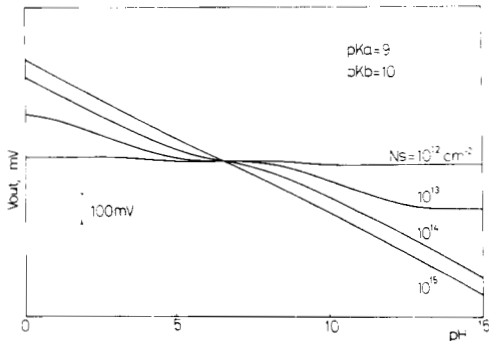


Fig. 2. The calculated pH response based on the Site-Binding Model of the proton dissociation on the metal oxide, where the acid dissociation constant  $pK_a$  is assumed 9 and the alkaline dissociation constant  $pK_b$  is assumed 10. The hydrogen dissociation site density  $N_s$  is taken as parameter. The equivalent gate voltage difference is a function of  $N_s$  and is linear to pH when  $N_s$  is increased.

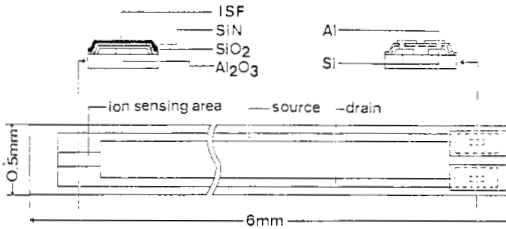


Fig. 3. Top and cross-sectional views of ISFET fabricated with silicon films on sapphire wafers. SOS structure is useful to prevent the electrical leakage between the side wall of the device and the electrolyte. The long source and drain regions are required to isolate the source and drain terminals from the electrolyte.

$$\begin{aligned} \text{pH} &= \{\log f(\theta_+) - \log \theta_+\}/2 \\ &+ (FNse/RTCH \ln 10)\{f(\theta_+) - \theta_+\} \end{aligned} \quad (5)$$

$$+ (pK_a + pK_w - pK_b) \quad (5)$$

$$= Nse\{\theta_+ - f(\theta_+)\}/(C_H) + C_1 \quad (6)$$

where  $\theta_+$ ,  $f(\theta_+)$ , and  $C_1$  are referred to in (A-1), (A-11), and (A-17) of the Appendix.  $N_s$  is the total number of hydroxyl groups on the oxide surface.

Then, Fig. 2 shows the calculated result by using (5) and (6), where  $pK_a = 9$ ,  $pK_b = 10$ , and  $N_s$  is changed as a parameter. It can be seen that the interface potential dependence upon pH becomes linear with an increase of  $N_s$ . The slope approaches to the Nernst response (60 mV/pH at 25°C) with increasing  $N_s$ .

### III. EXPERIMENTAL PROCEDURE

#### A. Fabrication of the ISFET

The fabrication step is similar to the process of the p-channel metal gate MOSFET's. As shown in Fig. 3, ISFET's are made by SOS's. The n-type Si film is 1  $\mu\text{m}$  in thickness and the resistivity is  $1 \Omega \cdot \text{cm}$ . The chip size is 0.5 mm in width, 6 mm in length, and 0.32 mm in thickness. The SOS-ISFET is a p-channel enhancement mode device, whose channel is 50  $\mu\text{m}$  long and 1400  $\mu\text{m}$  wide. The gate  $\text{SiO}_2$  film is thermally

TABLE I  
DETAILS OF BUFFER SOLUTION FOR pH MEASUREMENTS

	pH (25 °C)	Buffer solution
Standard	2.15	Tartrate
	4.01	Phthalate
	6.86	Phosphate
	9.18	Borate
	10.02	Alkaline Phosphate
Mixture	1.0-10.0	Clark-Lubs

TABLE II  
THE VALUE OF ACID DISSOCIATION CONSTANT, ALKALINE DISSOCIATION CONSTANT, HYDRATED CONSTANT, AND SURFACE SITE DENSITY

$\text{pK}_a$	$\text{pK}_b$	$(\text{pK}_a + \text{pK}_w - \text{pK}_b)/2$		$\text{pK}_{\text{OH}}$	$N_s (\text{cm}^{-2})$	
		A	B		A	B
$\text{SiO}_2$	13	10	—	6	—	9
$\text{ZrO}_2$	18.8	19	12.8	9	10	12
$\text{Ta}_2\text{O}_5$	9.6	9	13	10	5.3	6.5

A : theoretical value or measured value

B : fitting value

grown on the surface of the substrate at 1000°C for 30 min. The  $\text{SiO}_2$  thickness is about 530 Å. The silicon nitride film is grown on the  $\text{SiO}_2$  film by plasma enhanced chemical vapor deposition (PCVD) at 400°C for 5 min and the  $\text{SiH}_4$  (4 percent  $\text{N}_2$  base) gas pressure of 0.2 torr. The power is 0.4 W/cm<sup>2</sup>, the electrode separation is 38 mm, and the frequency is 13.56 MHz. The silicon nitride film thickness is about 500 Å. An ion-sensing film (ISF) is grown on the silicon nitride film as follows:

1)  $\text{SiO}_2$ :  $\text{SiO}_2$  films are made by the plasma anodic oxidation [19] of silicon nitride at the substrate temperature of 450°C and oxygen pressure of 0.1 torr. The thickness is approximately 20 nm.

2)  $\text{ZrO}_2$ : Zr films are evaporated by electron beam at the pressure of  $5 \times 10^{-7}$ - $10^{-8}$  torr. The purity of Zr source is 99.9 percent. Then a  $\text{ZrO}_2$  film is made by the plasma oxidation of this Zr film at the substrate temperature of 100°C and oxygen pressure of 0.2 torr. The power is 0.4 W/cm<sup>2</sup>, the electrode separation is 38 mm, and the frequency is 13.56 MHz. The thickness is approximately 40 nm.

3)  $\text{Ta}_2\text{O}_5$ :  $\text{Ta}_2\text{O}_5$  films are made by sputtering the  $\text{Ta}_2\text{O}_5$  target (purity of 99.99 percent) at the substrate temperature of 20°C and argon pressure of 0.1 torr. The thickness is approximately 100 nm.

#### B. Measurement of the Response

In order to measure the electrochemical response of the ISF, all measurements were done in the dark at the constant temperature. A feedback circuit was used to keep the drain voltage  $V_d$  and the drain current  $I_d$  constant by varying the gate voltage to compensate the interface potential change. The gate voltage was applied through a double junction type calomel electrode (Orion double junction type 90-02) immersed in the following buffer solution (Table I).

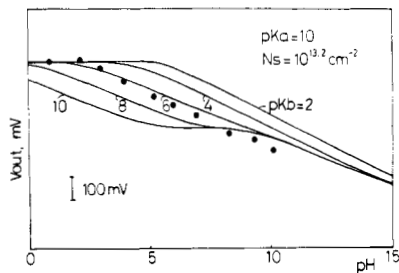


Fig. 4. Interface potential versus pH relationship of the  $\text{SiO}_2$ -gate ISFET's. Solid lines indicate the results of the calculation based on the Site-Binding Model of the proton dissociation reaction on the  $\text{SiO}_2$  surface. The experimental pH response is shown with circles ( $pK_a = 10$ ,  $pK_b = \text{parameter}$ ,  $N_s = 10^{13.2} \text{ cm}^{-2}$ ). The experimental results are in good agreement with the calculated result for  $pK_b = 6$ .

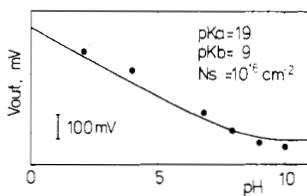


Fig. 5. Interface potential versus pH relationship of the  $\text{ZrO}_2$ -gate ISFET's. The solid line indicates the results of the calculation based on the site-binding model of the proton dissociation reaction on the  $\text{ZrO}_2$  surface. The experimental pH response is shown with circles. The experimental results are in good agreement with the calculated result for  $pK_a = 19$ ,  $pK_b = 9$ , and  $N_s = 10^{16} \text{ cm}^{-2}$ .

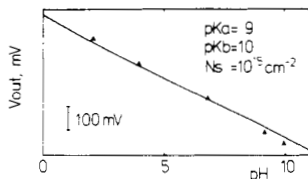


Fig. 6. Interface potential versus pH relationship of the  $\text{Ta}_2\text{O}_5$ -gate ISFET's. Solid line indicates the results of the calculation based on the Site-Binding Model of the proton dissociation reaction on the  $\text{Ta}_2\text{O}_5$  surface. The experimental pH response is shown with triangles. The experimental results are in good agreement with the calculated result for  $pK_a = 9$ ,  $pK_b = 10$ , and  $N_s = 10^{15} \text{ cm}^{-2}$ .

Standard buffer solution shown in Table II were used together with mixed buffer solution of Clark-Lubs. The values of pH were measured by pH meter (Orion Ion Analyzer 901), which was calibrated by standard buffer solution.

#### IV. EXPERIMENTAL RESULTS AND DISCUSSION

The pH sensitivities of various ISFET's are shown in Figs. 4, 5, and 6.

##### A. $\text{SiO}_2$ -Gate ISFET

The  $\text{SiO}_2$ -gate ISFET gives relatively small pH sensitivity (approximately 43 mV/pH) and it varies by the hydrogen-ion activity of the electrolyte. Furthermore, the sensitivity is not stable and a large long-term drift is observed in alkaline buffer solution (8–20 mV/h). Therefore, the pH value measured after 30 min from the time of changing the hydrogen-ion activity are indicated with circles. The lines in Fig. 4 indicate the

results of calculation based on the site-binding model of the proton dissociation reaction on the  $\text{SiO}_2$  surface. (The value of  $pK_a = 10$  is adopted as the value of the silicic acid in the water [20]. No data of  $pK_b$  is available, so  $pK_b$  is taken as a parameter.)

The value of surface site concentration,  $N_s$  is calculated from (A3),  $N_s = K_{\text{OH}} \times N_{ss}$ , where  $N_{ss}$  is the total number of the surface site group. For example, in the case of  $\text{SiO}_2$ ,  $\text{SiO}_2$  reacts with water to form the silanol site,  $\text{SiOH}$ . The silanol site,  $\text{SiOH}$  becomes  $\text{SiO}^-$  or  $\text{SiOH}_2^+$  depending on the hydrogen ion activity of the electrolyte. The surface density of Si on  $\text{SiO}_2$  is approximately  $10^{15} \text{ cm}^{-2}$  and the equilibrium constant  $K_{\text{OH}}$  is approximately  $10^{-1.8}$ .  $K_{\text{OH}}$  is given by

$$K_{\text{OH}} = H_2\text{SiO}_3/\text{SiO}_2 \times \text{H}_2\text{O}. \quad (7)$$

So the hydrogen-dissociation-site density  $N_s$  is given by

$$\begin{aligned} N_s(\text{SiO}_2) &= 10^{15} \times 10^{-1.8} \\ &= 10^{13} \text{ cm}^{-2}. \end{aligned} \quad (8)$$

Now, the acid dissociation constant ( $pK_a = 10$ ) and the alkaline dissociation constant ( $pK_b = 2, 4, 6, 8, 10$ ) are substituted into (5) and (6) to calculate the interface potential. The good agreement between experimental data and theoretical data is obtained at  $pK_b = 6$ .

Acid dissociation constant, alkaline dissociation constant, and the hydrated constant which are used on the calculation are shown in Table I.

##### B. $\text{ZrO}_2$ -Gate ISFET

The  $\text{ZrO}_2$ -gate ISFET shown in Fig. 5 has a better pH sensitivity than the  $\text{SiO}_2$ -gate ISFET. Its sensitivity is approximately 50 mV/pH. But,  $\text{ZrO}_2$ -gate ISFET shows a very slow response to a change of the hydrogen-ion activity and requires almost 10 min to get 90-percent response. Because the value of  $pK_{\text{OH}}$  is negative for  $\text{ZrO}_2$  [21], all the surface is hydrated and becomes  $\text{Zr}(\text{OH})_2$ , when  $\text{ZrO}_2$  is immersed into the water.  $\text{ZrO}_2$  is supposed to be hydrated by about ten atomic layers from the surface and the actual hydrogen-ion-dissociation-site density may be estimated about  $10^{16} \text{ cm}^{-2}$ . Also included in Fig. 5 is a theoretically computed pH response obtained using the parameters  $pK_a = 18$ ,  $pK_b = 11$ , and  $N_{ss} = 10^{16} \text{ cm}^{-2}$ .

##### C. $\text{Ta}_2\text{O}_5$ -Gate ISFET

The  $\text{Ta}_2\text{O}_5$ -gate ISFET shown in Fig. 6 has the highest pH sensitivity of 56 mV/pH among the three. When the hydrogen-ion activity of the electrolyte is changed, for example, from pH 2 to pH 10 and from pH 10 to pH 2 abruptly, the 90-percent response time is 2.4 and 0.7 s, respectively. Because there are no data of  $pK_{\text{OH}}$  for  $\text{Ta}_2\text{O}_5$ , we assumed zero for  $pK_{\text{OH}}$ . A theoretically computed pH response obtained using the parameters  $pK_a = 9$ ,  $pK_b = 11$ , and  $N_{ss} = 10^{15} \text{ cm}^{-2}$  is also included in Fig. 6.

From the results mentioned above, the most suitable material for hydrogen-ion measuring (from pH = 0 to pH = 10) must have the value of  $(pK_a + pK_w - pK_b)/2$  which is around 5 and the value of  $N_s$  which is about  $10^{15} \text{ cm}^{-2}$ .

## V. CONCLUSION

SOS structures have been successfully used to fabricate ISFET's with  $\text{SiO}_2$ ,  $\text{ZrO}_2$ , or  $\text{Ta}_2\text{O}_5$  as hydrogen-ion-sensing film. The  $\text{SiO}_2$ -gate ISFET gives relatively small pH sensitivity of 43 mV/pH and has a long-term drift of 8 to 20 mV/h. The  $\text{ZrO}_2$ -gate ISFET gives the pH sensitivity of 50 mV/pH, but shows a very slow response (90-percent response time is 10 min). The  $\text{Ta}_2\text{O}_5$ -gate ISFET has the highest pH sensitivity of 56 mV/pH and its 90-percent response time is a few seconds. Therefore,  $\text{Ta}_2\text{O}_5$  film is concluded to be the most suitable as the sensing material of ISFET's for measuring the hydrogen activity of the electrolyte. The results of calculation based on the site-binding model of the proton dissociation reaction on the metal oxide film are in good agreement with the experimental data of pH sensitivity. This model will be useful for searching the material that is sensitive to hydrogen ions.

## APPENDIX

Following the procedure given by Nakashima *et al.* [22], the hydrogen-ion activity can be represented in terms of the surface coverage by charged groups, the surface electrostatic potential, and the acid and alkaline dissociation constants.

The total number of hydroxyl groups on the oxide surface  $N_s$  depends on the hydrated constant and the material characteristics. Letting the percentage of the positively charged group be  $\theta_+$  and negatively charged group be  $\theta_-$  we then obtain the following equations:

$$\theta_+ = \nu_{\text{MOH}_2^+}/N_s \quad (\text{A1})$$

$$\theta_- = \nu_{\text{MO}^-}/N_s \quad (\text{A2})$$

$$N_s = K_{\text{OH}} N_{ss}$$

$$= \nu_{\text{MOH}_2^+} + \nu_{\text{MO}^-} + \nu_{\text{MOH}} \quad (\text{A3})$$

where

- $\nu_A$  equilibrium number of A's species per unit area,
- $N_s$  hydrogen-dissociation-site density,
- $K_{\text{OH}}$  hydrated constant, and
- $N_{ss}$  total number of surface group which is OH group on the surface of the metal oxide.

Total surface charge per unit area  $\sigma_0$  is given by

$$\sigma_0 = Nse(\theta_+ - \theta_-) \quad (\text{A4})$$

where  $e$  equals electronic charge ( $-1.6 \times 10^{-19}$  C).

Using the acid dissociation constant  $Ka$  and the alkaline dissociation constant  $Kb$ , the electrochemical equations (3) and (4) can be rewritten as

$$Ka = \exp \{(\mu_{\text{MOH}^-}^0 - \mu_{\text{MO}^-}^0 - \mu_{M^+}^0)/kT\} \quad (\text{A5})$$

$$Kb/Kw = \exp \{(\mu_{\text{MOH}}^0 + \mu_{H^+}^0 - \mu_{\text{MOH}_2^+}^0)/kT\} \quad (\text{A6})$$

where

- $\mu_A^0$  standard chemical potential of A's species,
- $k$  Boltzmann's constant,
- $T$  absolute temperature, and
- $Kw = H^+ \times OH^-$  water constant.

Combining (3), (4), (A1), (A2), (A3), (A4), (A5), and (A6) yield

$$\theta_+ \theta_- / (1 - \theta_+ - \theta_-)^2 = Ka Kb / Kw \quad (\text{A7})$$

$$\begin{aligned} \theta_+ / \theta_- &= (a_{\text{H}^+}^2 + Ka / Kw Kb) \\ &\times \exp(-2e\varphi/kT) \end{aligned} \quad (\text{A8})$$

where  $a_{\text{H}^+}$  is the hydrogen-ion activity and  $\varphi$  is interface potential between the electrolyte and the oxide.

Solving the equation (A8) for  $a_{\text{H}^+}$ , we obtain

$$\begin{aligned} -\log a_{\text{H}^+} &= (\log \theta_- - \log \theta_+)/2 \\ &- F/RT \ln 10 \\ &+ (-\log Ka - \log Kw + \log Kb)/2 \end{aligned} \quad (\text{A9})$$

where  $R$  is gas constant and  $F$  is Faraday constant.

By substituting (2) into (A9)

$$\begin{aligned} -\log a_{\text{H}^+} &= (\log \theta_- - \log \theta_+)/2 + (F/RT \ln 10) \\ &\times \{-\sigma_0 + C_0(V_s - V^*)\}/(C_0 + C_H) \\ &+ (-\log Ka - \log Kw + \log Kb)/2 \end{aligned} \quad (\text{A10})$$

is obtained. Then, in (A7), we are left with

$$\begin{aligned} \theta_- &= f(\theta_+) \\ &= (Kw/2KaKb - 1) \times \theta_+ + 1 \\ &- \sqrt{(Kw\theta_+/KaKb) \times \{(Kw/KaKb - 4)\theta_+ + 4\}}/2. \end{aligned} \quad (\text{A11})$$

The substitution of (A11) to (A10) yields

$$\begin{aligned} \text{pH} &= \{\log f(\theta_+) - \log \theta_+\}/2 \\ &+ [FNse\{f(\theta_+) - \theta_+\}]/[RT \ln 10(C_0 + C_H)] \\ &+ FC_0(V_s - V^*)/[RT \ln 10(C_0 + C_H)] \\ &+ (pKa + pKw - pKb)/2 \end{aligned} \quad (\text{A12})$$

where

- $C_0$  capacitance per unit area of oxide film,
- $C_H$  capacitance per unit area of the electronic double layer, and
- $V_{\text{ref}}$  reference electrode potential.

The interface potential  $\varphi$  is given

$$\begin{aligned} \varphi &= \Phi_0 - V^* \\ &= Nse\{\theta_+ - f(\theta_+)\}/(C_H + C_0) \\ &- C_0(V_s - V^*)/(C_H + C_0) \end{aligned} \quad (\text{A13})$$

where

- $\Phi_0$  potential of the oxide surface,
- $V^* = V_g - V_{\text{ref}} + E^0 + (RT/F) \ln a_{\text{H}^+}$ ,
- $V_g$  biased gate potential,
- $E^0$  standard electrolyte potential, and
- $V_s$  potential of silicon substrate.

Substituting  $V = V_g - V_{\text{ref}} + E^0 - RT(\ln 10)pH/F$  into (A12)

and (A13),  $pH$  and are represented as functions of  $\theta_+$  as indicated below

$$\begin{aligned} pH(\theta_+) = & \left(1 + \frac{C_0}{C_H}\right) \left[ \frac{\log f(\theta_+) - \log \theta_+}{3} \right. \\ & \left. + \frac{FN_s e \{f(\theta_+) - \theta_+\}}{(C_H + C_0) RT \ln 10} + \frac{pKa + pKb - pKw}{2} \right] \\ & + \frac{C_0}{C_H} \frac{F}{RT \ln 10} (V_s - V_g + V_{ref} - E^0) \end{aligned} \quad (A14)$$

$$\begin{aligned} \varphi(\theta_+) = & \frac{N_s e \{\theta_+ - f(\theta_+)\}}{C_H + C_0} + \frac{C_0}{C_H} \frac{RT \ln 10 pH(\theta_+)}{F} \\ & + \frac{C_0}{C_H} (V_s - V_g + V_{ref} - E^0). \end{aligned} \quad (A15)$$

These equations can be simplified as follows:

$$\varphi(\theta_+) = N_s e \{\theta_+ - f(\theta_+)\}/C_H + C_1 \quad (A16)$$

$$C_1 = C_0 (V_s - V_g + V_{ref} - E^0)/C_H. \quad (A17)$$

By assuming -4.5 V as  $V \cdot s$ , 0.24 V as  $V_{ref}$ , -4.5 V as  $E^0$ , 1.0 V as  $V_g$ , taking in account that  $C_H$  is of the order of 10  $\mu\text{F/cm}^2$  and  $C_0$  is the order of 30 nF/cm<sup>2</sup>,  $pH$  and interface potential are given by (5) and (6).

#### ACKNOWLEDGMENT

The authors are indebted to Dr. H. Shiraki, K. Sakuma, and Dr. T. Kuriyama, Central Research Laboratories, Nippon Electric Company, for their helpful discussions.

#### REFERENCES

- [1] P. Bergveld, "Developments of ion-sensitive solid-state device for neuro-physiological measurements," *IEEE Trans. Biomed. Eng.*, vol. BME-17, pp. 70-71, Jan. 1970.
- [2] —, "Developments, operation, and application of the ion-sensitive field-effect transistor as a tool for electrophysiology," *IEEE Trans. Biomed. Eng.*, vol. BME-19, pp. 342-351, Sept. 1972.
- [3] T. Matsuo and K. D. Wise, "An integrated field-effect electrode for biopotential recording," *IEEE Trans. Biomed. Eng.*, vol. BME-21, pp. 485-487, Nov. 1974.
- [4] R. P. Back and D. E. Hackleman, "Field effect potentiometric sensors," *Anal. Chem.*, vol. 49, pp. 2315-2321, 1977.
- [5] S. D. Moss, J. Janata, and C. C. Johnson, "Potassium ion-sensitive field effect transistor," *Anal. Chem.*, vol. 47, pp. 2238-2243, 1975.
- [6] J. Janata and S. D. Moss, "Chemically sensitive field effect transistors," *IEEE Trans. Biomed. Eng.*, vol. BME-23, pp. 241-245, July 1976.
- [7] P. Bergveld, J. Wiersma, and H. Meertens, "Extracellular potential recording by means of a field effect transistor without gate metal, called OSFET," *IEEE Trans. Biomed. Eng.*, vol. BME-23, pp. 136-144, Mar. 1976.
- [8] J. N. Zemel, "Ion-sensitive field effect transistors and related devices," *Anal. Chem.*, vol. 47, pp. 255A-268A, Feb. 1975.
- [9] R. P. Buck and D. E. Hackleman, "Field effect potentiometric sensors," *Anal. Chem.*, vol. 43, pp. 2315-2321, 1977.
- [10] I. R. Lauks, "pH measurements using polarizable electrodes," *IEEE Trans. Electron Devices*, vol. ED-26, pp. 1952-1959, Nov. 1979.
- [11] A. G. Revesz, "On the mechanism of the ion sensitive field effect transistor," *Thin Solid Films*, vol. 41, pp. 643-647, Mar. 1977.
- [12] P. Bergveld, N. F. deRooij, and J. N. Zemel, "Physical mechanisms for chemically sensitive semiconductor devices," *Nature*, vol. 273, pp. 438-443, 1978.
- [13] I. R. Lauks and J. N. Zemel, "The Si<sub>3</sub>N<sub>4</sub>/Si ion sensitive semiconductor electrode," *IEEE Trans. Electron Devices*, vol. ED-26, pp. 1959-1964, Dec. 1979.
- [14] W. M. Siu and R. S. C. Cobbold, "Basic properties of the electrolyte-SiO<sub>2</sub>-Si system: Physical and theoretical aspects," *IEEE Trans. Electron Devices*, vol. ED-26, pp. 1805-1814, Nov. 1979.
- [15] H. Abe, M. Esashi, and T. Matsuo, "ISFET's using inorganic gate thin films," *IEEE Trans. Electron Devices*, vol. ED-26, pp. 1939-1944, Dec. 1979.
- [16] S. D. Moss, C. C. Johnson, and J. Janata, "Hydrogen, calcium, and potassium ion-sensitive FET transducers: A preliminary report," *IEEE Trans. Biomed. Eng.*, vol. BME-25, pp. 49-54, Jan. 1978.
- [17] J. W. Perram, R. J. Hunter, and H.J.L. Wright, "The oxide-solution interface," *Aust. J. Chem.*, vol. 27, pp. 461-475, 1974.
- [18] D. E. Yates, S. Levire, and T. W. Healy, "Site-binding model of the electrical double layer at the oxide/water interface," *J. Chem. Soc., Faraday Trans.*, vol. 1, no. 70, pp. 1807-1818, 1974.
- [19] V. Q. Ho and T. Sugano, "Selective anodic oxidation of silicon in oxygen plasma," *IEEE Trans. Electron Devices*, vol. ED-27, pp. 1436-1443, Aug. 1980.
- [20] A. Paul and A. Youssefi, "Alkaline durability of some silicate glasses containing CaO, FeO and MnO," *J. Mat. Sci.*, vol. 13, pp. 97-107, 1978.
- [21] A. Poult, "Chemical durability of glasses: A thermodynamic approach," *J. Mat. Sci.*, vol. 12, pp. 2246-2268, 1977.
- [22] H. Nakajima, M. Esashi, and T. Matsuo, "The pH-response of organic gate ISFET's and the influence of macro-molecule adsorption," *Nippon Kagaku Kaishi* (in Japanese), pp. 1499-1508, 1980.